Shahrood University of Technology

Journal of Hydraulic and Water Engineering (JHWE)

Journal homepage: https://jhwe.shahroodut.ac.ir/

Iranian Hydraulic Association (IHA)

Calculation of Hydrodynamics Resistance Coefficient of Diver by CFD Method

N. Khanmoradi [1,*], S. Jafari Horestani [2], M. Moonesun [3]

[1] Department of Mechanical Engineering, Sharif University of Technology, Tehran, Iran.
[2] Department of Physical Education and Sport Sciences, Kharazmi University, Tehran, Iran.
[3] Department of Civil Engineering, Shahrood University of Technology, Shahrood, Iran

Article Info

Article history:

Received: 25 March 2023
Received in revised form: 21 May 2023
Accepted: 15 June 2023
Published online: 15 August 2023

DOI:
10.22044/JHWE.2023.12878.1010

Keywords:
Human body
Swimmer resistance
CFD
Resistance coefficient

Abstract

The purpose of the present study is calculation of the resistance and resistance coefficient of a diver at underwater swimming. One of the results of this article is useful for designing different types of thrusters. This study uses a computational fluid dynamics methodology. SST k-omega turbulent model is implemented in the Star-CCM+ application and is applied to the flow around a three-dimensional model of an adult human bare hull. Three common swimming positions are investigated in an adult swimmer: a ventral position with the arms extended at the front, a ventral position with the arms placed alongside the trunk and a ventral position with one arm extended at the front and another arm placed alongside the trunk. The simulations are applied to flow velocities between 0.5 and 2.25m/s with increasing step of 0.25m/s, which are typical speed of swimmers. According to the resistance coefficient vs Reynolds number diagrams, submerged diving with two hands alongside the trunk is the best way of diving with lower resistance.

1. Introduction

Resistance and resistance coefficient in different velocities during surface and near surface swimming (two phases) for three usual positions of swimming is calculated by CFD method (Khanmoradi et al., Under Revision-a). This article says that how different positions of diving affect on resistance and resistance coefficient based on cross-section area and wetted area. Also, there is similar study for a diver with diving equipment by Khanmoradi that shows how diving equipment contribute to increasing the resistance of diver during the swimming (Khanmoradi et al., Under Revision-b).

The passive resistance of male swimmer moving underwater in a streamlined position has been measured experimentally (for example, (Bixler et al., 2007); (Costa et al., 2011)). Their results suggest that a three-dimensional computational fluid dynamics analysis of a human form could provide useful information about swimming.

Swimming performance is determined by the combined effect of propulsion, drag and technical skill (Chatard et al., 1990). Passive

* ☒ *Corresponding author:* nimakhanmoradi.edu@gmail.com, Tel:+989905014283

drag, it can be considered as a relevant predictor of gliding performance during the underwater phases of the starts and turns, which are important components of the overall swimming event (D'Acquisto, 1988). Lyttle et al. (1998) found the reduction of the hydrodynamic resistance during the glide leads to reduces turning times. The most common method used to study the passive drag acting in human swimming is by towing subjects at various velocities, body positions and depths using electro-mechanical motors or weights and pulley systems (for example, (Counsilman and Recreation, 1955); (Kolmogorov et al., 1997); (Lyttle et al., 2000); (Toussaint et al., 2004)). However, other methods are being used, like the Inverse Dynamics (Vilas-Boas et al., 2010) and CFD ((Bixler et al., 2007); (Zaidi et al., 2008); (Marinho et al., 2009)). The CFD method is a numerical modelling technique that can be applied to hydrodynamic phenomena, and is used as an alternative approach to the experimental research regarding the determination of a swimmer's passive drag (Mantha et al., 2014). Also, the effect of depth is checked with a three-dimensional method (Novais et al., 2012). The resistance coefficient for underwater vehicles is calculated (Liu et al., 2021).

All the existing researches are devoted to providing the resistance of the swimmer's body in streamline form, which is analyzed in the swimming pool. In the meantime, there is a gap in comprehensive research regarding the body resistance of a diver or swimmer with a non-streamline body shape in the sea. There are many marine propulsion devices and systems that are used to facilitate the movement of swimmers and divers. These devices have both recreational and military aspects. Many of them are used only for the movement of ordinary people without diving equipment, and many of them are used to facilitate the movement of divers in military affairs (Figure 1).

Figure 1. Different Types of Underwater Scooters (dive-hurghada., (n. d.)); (finish-tackle., (n. d.))

For an ideal design of these devices, the upcoming research will be very useful. Therefore, by considering the available types of thrusters, the different states of a diver's body have been created in CAD (Computer-Aided Design) and the amount of resistance coefficient has been obtained.

2. Data, Methods and Models

2.1. Three-Dimensional Model

To obtain the geometry of a human body, a bare body model of an adult real human was created in CAD. The basic swimmer's mode used for the analysis with dimensions and head, chest, waist, and hip circumferences, is shown in Figure 2.

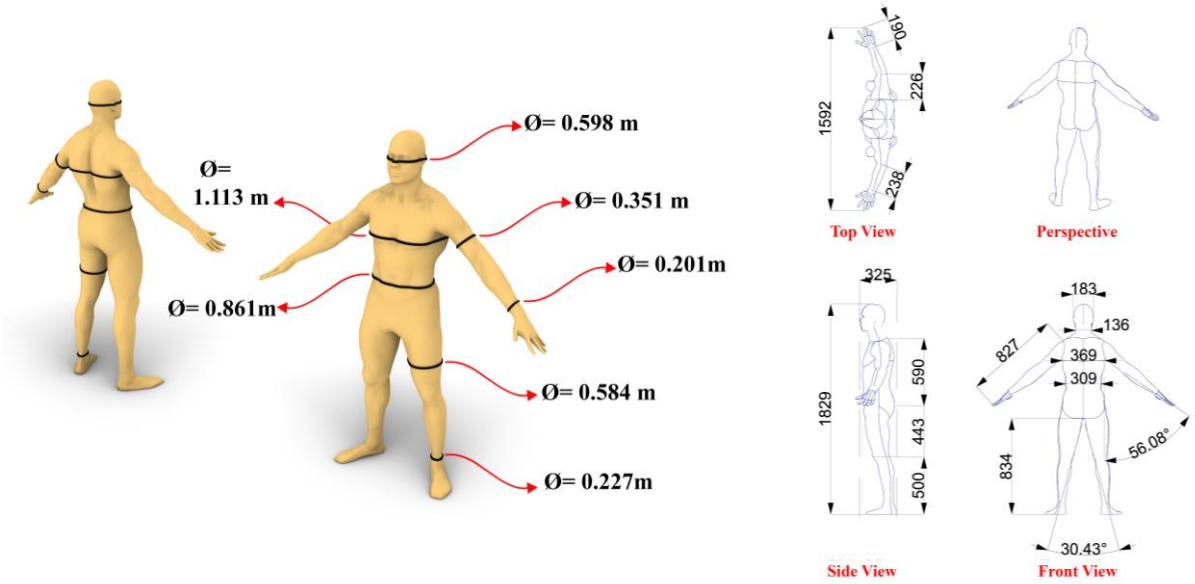

Figure 2. Main Geometry Dimension and Specification

First, an initial streamline geometry is created to allow validation with existing articles. Then, according to the different models of thrusters, the different positions are extracted from the main geometry (Figure 2). The geometry number 1, the body shape of a normal swimmer in a ventral position with the arms extended at the front, to use a two-handed thruster, geometry number 2, in a ventral position with the arms placed alongside the trunk and geometry number 3, a combination of two geometries 1 and 2 in a ventral position with one arm extended at the front and another arm placed alongside the trunk which are practically suitable for designing of single handle thrusters. The frontal projected area for geometry 1 to 3 are 0.108, 0.142 and 0.125 m2 respectively. These areas are calculated by projecting all cross sections on a surface in front and considering the maximum area. Also, the wetted areas are 2.111, 2.073 and 2.092 m2.

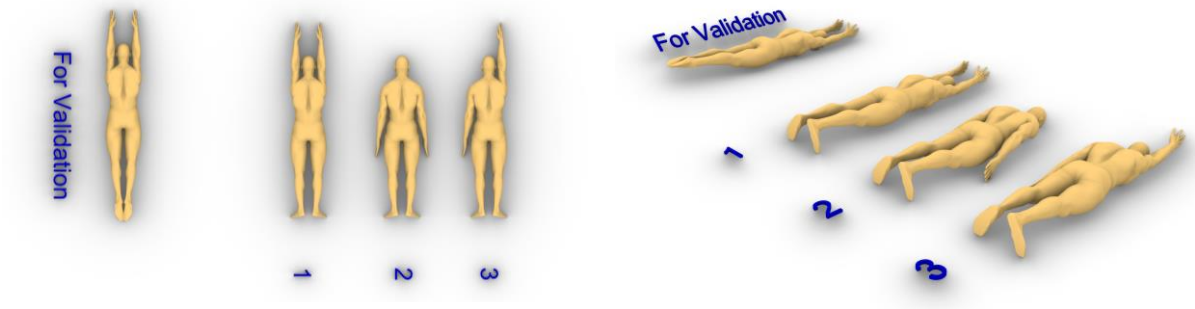

Figure 3. All analyzed geometry in one sight

2.2. Validation for CFD Simulation

As the first step of numerical simulation, it's necessary to valid our simulation with another articles. Therefore, CFD results of Bixler article (Bixler et al., 2007) are considered for validation process. A streamline geometry has been created with projected area near to the Bixler article. This

geometry that is shown in Figure 3, has used just for validation. Below table is a general comparison between geometry used in Bixler article and the geometry in this study.

Table 1. A comparison between the geometries used in this study and Bixler paper.

Parameter		B. Bixler	This Study
Lengths	Height	1.86 m	1.83
	Finger to Toe	2.34 m	2.4
Circumferences	Head	0.59 m	0.598
	Chest	1.02 m	1.113
	Waist	0.84 m	0.861
Areas	Frontal Projected Area	0.0934 m2	0.0997 m2
	Total Surface Area (Wet Surface)	1.859 m2	2.084 m2

Our validation results are shown in table below. The maximum error for validation based on resistance is about 9.4 percent and the maximum error based on resistance coefficient is about 2.49 percent that is acceptable. The higher errors for resistance are because of differences between the geometries. Based on this, we can continue our simulation for our new geometries.

Table 2. Validation Results.

	Speed	B. Bixler Results	This Study Results	Error (%)
Resistance	1.5	31.58	34.55	9.404
	1.75	42.74	46.64	9.125
	2	55.57	60.2952	8.503
	2.25	70.08	75.3096	7.462
Resistance Coefficient (Based on Projected Area)	1.5	0.3012	0.3087	2.4914
	1.75	0.2995	0.3061	2.2293
	2	0.2981	0.303	1.6468
	2.25	0.2971	0.299	0.6718

2.3. Main CFD Simulation

The CFD analysis are performed with the body in a horizontal position with an attack angle of 0°. The attack angle is defined as the angle between a horizontal line and a line drawn from the vertex to the ankle bone.

The boundary conditions of the computational fluid dynamics model are designed to represent the geometry and flow conditions of a part of a lane in the open water.

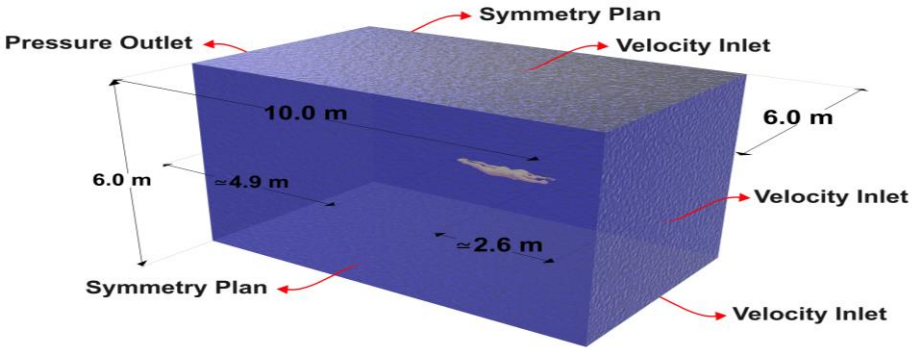

Figure 4. Domain and Boundary Condition.

Also, the swimmer model middle line is placed equidistant from the top and bottom surfaces. Domain dimensions and boundary condition are shown in Figure 4. We use a half of domain for symmetrical geometries to reduce cell numbers and time of each solving.

The grid is trimmed cell with prism layer. Significant efforts are conducted to ensure that the model would provide accurate results namely by decreasing the grid node separation in areas of high velocity and pressure gradients. Also, mesh independency is checked that results are shown in Figure 5 diagram.

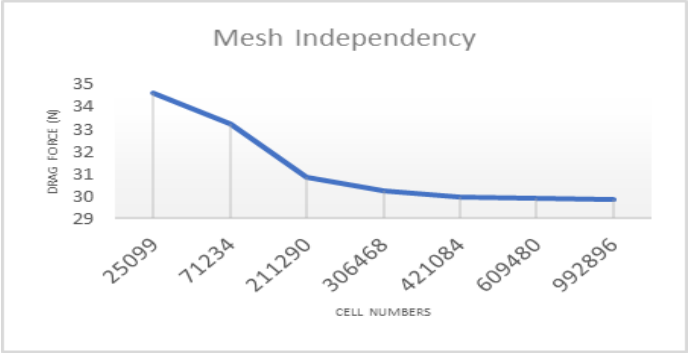

Figure 5. Mesh Study Diagram.

Based on the mesh study, we use about 421,000 cell numbers for the symmetry analysis. The implemented networking mesh on Geometry 1 is shown in Figure 6.

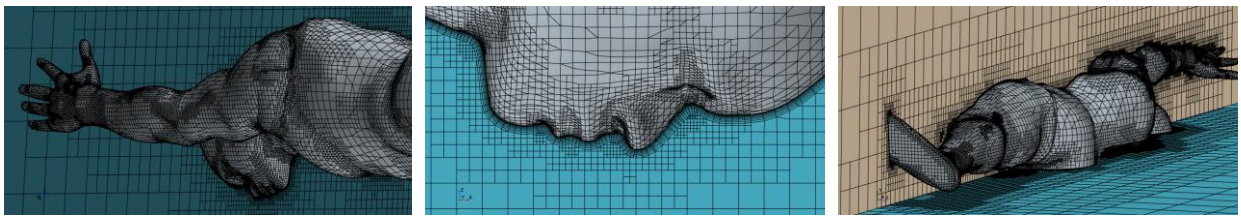

Figure 6. Trimmed Cell Mesh Implemented on Geometry no.1.

The main parameters of CFD simulation are shown in Table 3. In this table, solving parameters of our CFD simulations are shown in two parts of "Initial Conditions" and "Physics".

Table 3. Main Parameters of CFD Simulations.

Initial Conditions	**Roughness**	0
	Water Temperature	28 °C
	Water Density	997.561 kg/m^3
	Air Density	1.18415 kg/m^3
Physics	Three Dimensional	
	Single-Phase (Constant Density Water)	
	SST (Menter) K-Omega	
	Turbulence Suppression	
	Steady	
	Segregated Flow	
	Reynolds-Averaged Navier-Stokes	

We use the segregated solver with the standard SST k-omega turbulence model, because this turbulence model is shown to be accurate with measured values in another research (Moreira et al., 2006). The resistance coefficient is calculated for velocities ranging from 1.50 to 2.25 m/s in increments of 0.25 m/s that are equal with Reynolds number from 1035 to 5606. Flow velocities are chosen to be within the range of typical underwater swimming.

3. Results and Discussions

To analyze the relationship between the velocity and the resistance for different positions of swimming, diagram Figure 7 is extracted.

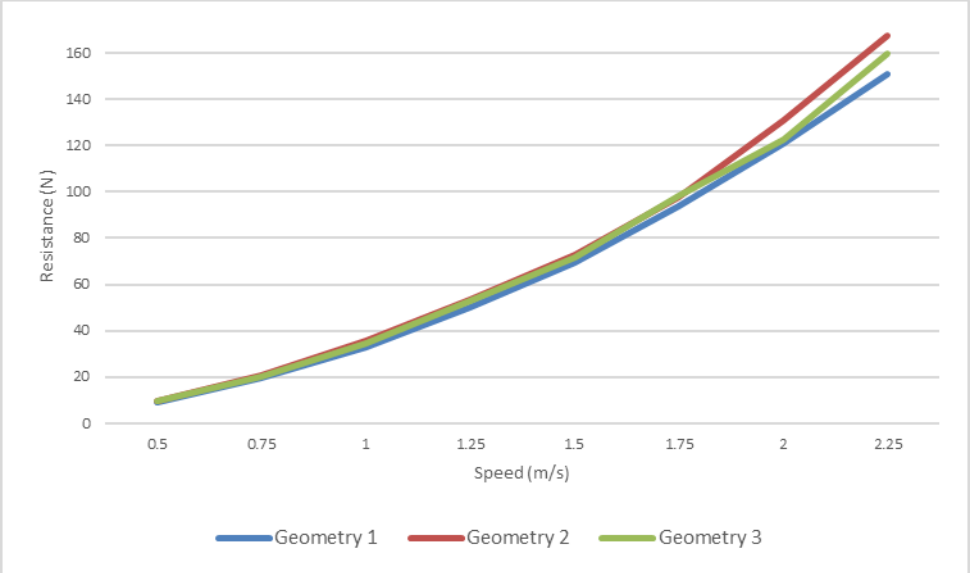

Figure 7. Resistance vs Speed Diagram for Different Swimming Positions.

The diagrams in Figure 8 show resistance coefficient vs Reynolds number for each geometry.

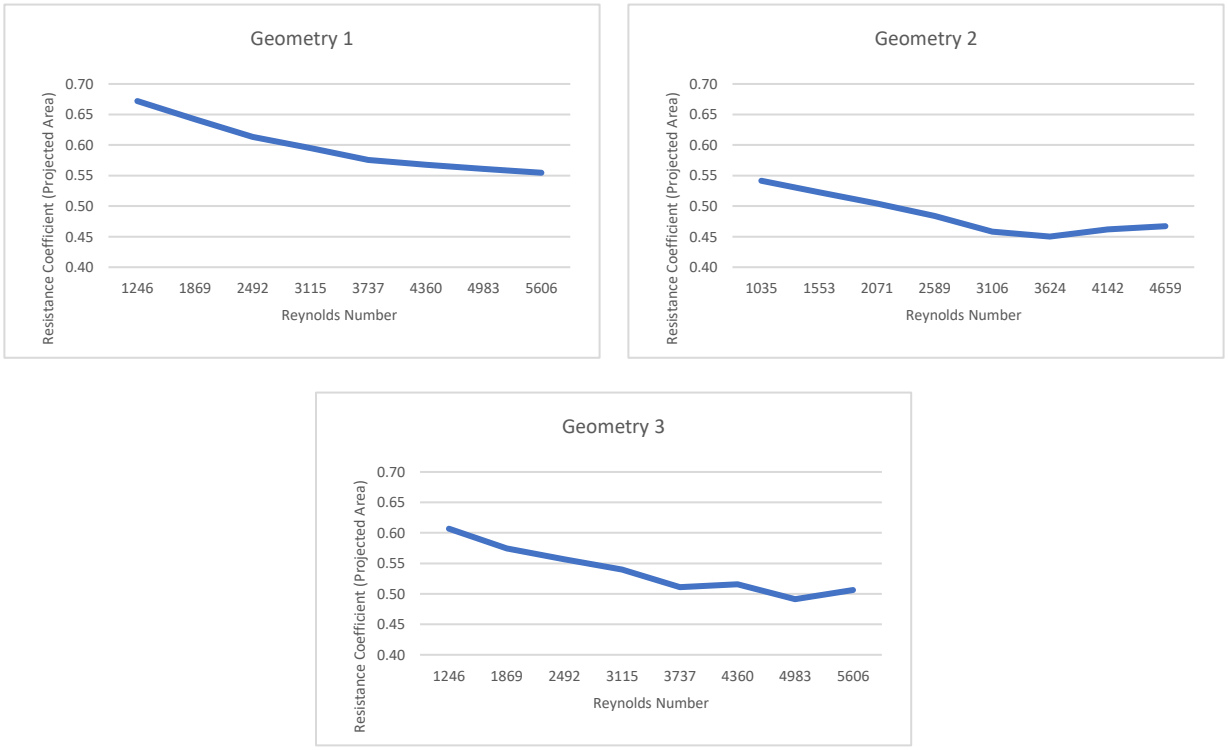

Figure 8. Resistance Coefficient vs Reynolds Number for Geometries no. 1 to 3.

For all the velocities, the resistance coefficient of the position with the arms extended at the front is lower than the resistance coefficient of the position with the arms along the trunk. Also, the geometry number 2 has resistance coefficient between geometries number 1 and 3.

4. Conclusion

The main aim of this study is to analyses the resistance coefficient arising from the use of three different positions in swimming, through computational fluid dynamics.

The resistance coefficient changes slightly from 0.672 at 1246 Reynolds to 0.5546 at 5606 Reynolds, in the position with the arms extended at the front, from 0. 0.6069 at 1246 Reynolds to 0.5064 at 5606 Reynolds number in the position with the arms along the trunk and finally from 0. 0.5415 at 1035 Reynolds to 0.4673 at 4659 Reynolds number, in position with one arm extended at the front and one arm alongside the trunk. The inverse relationship between the resistance coefficient and the velocity found in the current study seems to correspond to what happens in experimental situations with the human body totally submerged (Jiskoot and Clarys, 1975).

But about choosing the best body shape, the position with the arms extended at the front has lowest resistance coefficient in comparison with the other body positions in all speeds. The main reason of this results is because of higher cross-section area for geometry 3. Based on figure 3, hands have a little distance with the trunk and that leads to having increasing the cross-section area and also increasing the resistance and resistance

coefficient. Resistance of diver with different angles of hands can be calculated in future studies.

Although limited to resistance, this study allows the evaluation of the effects of different body positions on performance, being a first step toward the analysis of resistance. On the other hand, computational fluid dynamics methods have provided a way to estimate the relative contribution of each resistance component to the total resistance. Future studies could improve these computational fluid dynamics results by analyzing the resistance of a swimmer at the water's surface and including wave resistance in the measurements or also a study on effect of different equipment on swimming resistance.

Data Availability

The data used to support the findings of this study is available from the corresponding author upon request.

Conflicts of Interest

The authors declare that they have no conflicts of interest regarding the publication of this paper.

References

Khanmoradi, N., Moonesun, M., Jafari, H.S., Under Revision-a. Calculation of Hydrodynamics Resistance Coefficient of Diver by CFD Method at Free Surface, International Journal of Maritime Technology.

Khanmoradi, N., Moonesun, M., Jafari, H.S., Under Revision-b. Calculation of Hydrodynamics Resistance Coefficient of Diver with Diving Equipment by CFD Method, Ships and Offshore Structures.

Bixler, B., Pease, D., Fairhurst, F.J.S.b., 2007. The accuracy of computational fluid dynamics analysis of the passive drag of a male swimmer. 6(1): 81-98.

Costa, L.C. et al., 2011. Comparing computational fluid dynamics and inverse dynamics methodologies to assess passive drag during swimming gliding, ISBS-Conference Proceedings Archive.

Chatard, J., Lavoie, J., Bourgoin, B., Lacour, J.J.I.j.o.s.m., 1990. The contribution of passive drag as a determinant of swimming performance. 11(05): 367-372.

D'Acquisto, M., 1988. Breaststroke economy, skill and performance study of breaststroke mechanics, using a computer based" Velocity. Video" system. Zentrum f. Wissenschaftsinformation, Körperkultur u. Sport.

Lyttle, A.D., Blanksby, B.A., Elliott, B.C., Lloyd, D.G.J.J.o.S.R., 1998. The effect of depth and velocity on drag during the streamlined glide. 13.

Counsilman, J.E.J.R.Q.A.A.f.H., Physical Education, Recreation, 1955. Forces in swimming two types of crawl stroke. 26(2): 127-139.

Kolmogorov, S.V., Rumyantseva, O.A., Gordon, B.J., Cappaert, J.M.J.J.o.A.B., 1997. Hydrodynamic characteristics of competitive swimmers of different genders and performance levels. 13(1): 88-97.

Lyttle, A.D., Blanksby, B.A., Elliott, B.C., Lloyd, D.G.J.J.o.S.S., 2000. Net forces during tethered simulation of underwater streamlined gliding and kicking techniques of the freestyle turn. 18(10): 801-807.

Toussaint, H.M., Roos, P.E., Kolmogorov, S.J.J.o.b., 2004. The determination of drag in front crawl swimming. 37(11): 1655-1663.

Vilas-Boas, J.P. et al., 2010. Determination of the drag coefficient during the first and second gliding positions of the breaststroke underwater stroke. 26(3): 324-331.

Zaidi, H., Taiar, R., Fohanno, S., Polidori, G.J.J.o.B., 2008. Analysis of the effect of

swimmer's head position on swimming performance using computational fluid dynamics. 41(6): 1350-1358.

Marinho, D.A. et al., 2009. Hydrodynamic drag during gliding in swimming. 25(3): 253-257.

Mantha, V.R., Marinho, D.A., Silva, A.J., Rouboa, A.I.J.B.a.o.b., technology, 2014. The 3D CFD study of gliding swimmer on passive hydrodynamics drag. 57: 302-308.

Novais, M. et al., 2012. The effect of depth on drag during the streamlined glide: A three-dimensional CFD analysis. 33(2012): 55-62.

Liu, Y. et al., 2021. A fine drag coefficient model for hull shape of underwater vehicles. 236: 109361.

dive-hurghada., (n. d.). PADI Diver Propulsion Vehicle Specialty (Scooter). https://www.dive-hurghada.com/prices/padi-scuba-diving-courses/padi-diver-propulsion-vehicle-specialty.

finish-tackle., (n. d.). product., https://finish-tackle.com/product/magicjet-scooter/.

Jiskoot, J., Clarys, J.J.S.I., 1975. Body resistance on and under the water surface. 2: 105-109.

Appendix A

In this appendix, exact numbers of resistance, resistance coefficient based on wetted area and resistance coefficient based on frontal projected area for geometries no.1 to no.3 are presented.

Table A. 1. Amount of All Resistance and Resistance Coefficients.

	Velocity (m/s)	Resistance (N)	Resistance Coefficient (Projected Area)	Resistance Coefficient (wetted Area)
Geometry 1	V= 0.5 m/s	9.04	0.6720	0.0343
	0.75	19.44	0.6423	0.0328
	1	33	0.6133	0.0313
	1.25	50	0.5947	0.0304
	1.5	69.7	0.5757	0.0294
	1.75	93.56	0.5678	0.0290
	2	120.7	0.5608	0.0286
	2.25	151.08	0.5546	0.0283
Geometry 2	V= 0.5 m/s	9.58	0.5415	0.0371
	0.75	20.8	0.5226	0.0358
	1	35.68	0.5042	0.0345
	1.25	53.48	0.4837	0.0331
	1.5	73	0.4585	0.0314
	1.75	97.56	0.4502	0.0308
	2	130.8	0.4621	0.0316
	2.25	167.4	0.4673	0.0320
Geometry 3	V= 0.5 m/s	9.45	0.6069	0.0362
	0.75	20.13	0.5746	0.0343
	1	34.68	0.5568	0.0332
	1.25	52.56	0.5401	0.0322
	1.5	71.58	0.5108	0.0305
	1.75	98.33	0.5155	0.0308
	2	122.4	0.4913	0.0293
	2.25	159.66	0.5064	0.0302